IEEE Photonics Journal
An IEEE Photonics Society Publication

Open Access

Deep-Ultraviolet Emitting AlGaN Multiple Quantum Well Graded-Index Separate-Confinement Heterostructures Grown by MBE on SiC Substrates

Volume 9, Number 4, August 2017

Haiding Sun
Jian Yin
Emanuele Francesco Pecora
Luca Dal Negro
Roberto Paiella, *Senior Member, IEEE*
Theodore D. Moustakas, *Fellow, IEEE*

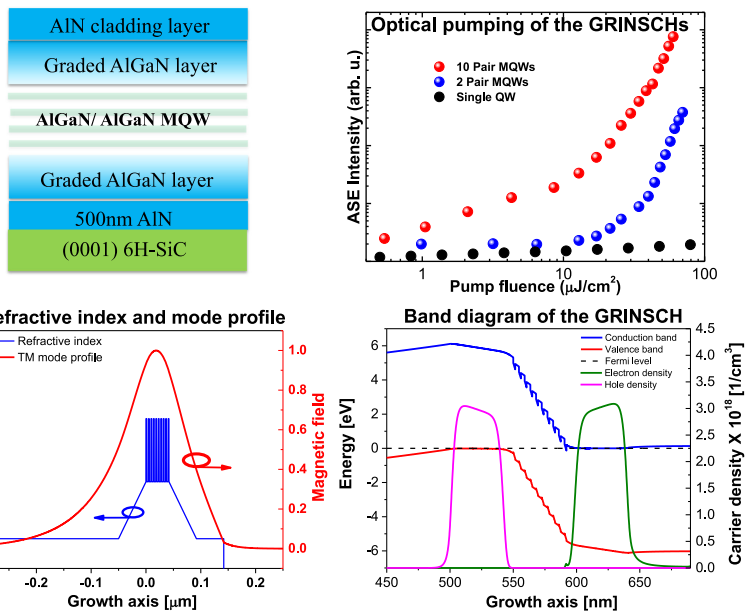

DOI: 10.1109/JPHOT.2017.2716420
1943-0655

Deep-Ultraviolet Emitting AlGaN Multiple Quantum Well Graded-Index Separate-Confinement Heterostructures Grown by MBE on SiC Substrates

Haiding Sun,[1] Jian Yin,[1] Emanuele Francesco Pecora,[1] Luca Dal Negro,[1,2] Roberto Paiella,[1,2] *Senior Member, IEEE*, and Theodore D. Moustakas,[1,2] *Fellow, IEEE*

[1]Department of Electrical and Computer Engineering and Photonics Center, Boston University, Boston, MA 02215 USA
[2]Division of Materials Science and Engineering , Boston University, Boston, MA 02215 USA

DOI:10.1109/JPHOT.2017.2716420

Manuscript received January 20, 2017; revised May 23, 2017; accepted June 13, 2017. Date of publication June 16, 2017; date of current version August 17, 2017. This work was supported in part by the NSF Division of Electrical, Communications and Cyber Systems under Standard Grant 1408364, overseen by Dr. M. Fallahi. Corresponding authors: Haiding Sun and Theodore D. Moustakas (e-mail: haiding@bu.edu; tdm@bu.edu).

Abstract: Deep-ultraviolet emitting structures based on $Al_{0.65}Ga_{0.35}N/Al_{0.8}Ga_{0.2}N$ multiple quantum wells (MQWs), embedded in compositionally graded $Al_xGa_{1-x}N$ films in the form of graded-index-separate-confinement heterostructure, were grown by molecular beam epitaxy. The graded AlGaN layer blocked threading defects (TDs) in the vicinity of the AlN/AlGaN heterointerface, resulting in a reduction of the TDs in the active layer. The intensity of the transverse-magnetic polarized amplified spontaneous emission spectra with peak emission at 270 nm was found to increase linearly with the number of QWs. Furthermore, while the peak intensity for devices with a single QW varies linearly with the pump fluence, it varies superlinearly for larger number of QWs, suggesting light amplification by stimulated emission. These results are consistent with numerical simulations, which indicate that the confinement of the optical mode in this device structure increases with the number of QWs and simultaneously the threshold under optical pumping decreases with increasing of the number of QWs. Finally, the band structure simulations indicate that the device is in the form of a p-n junction due to polarization-induced p- and n-doping in the compositionally graded $Al_xGa_{1-x}N$ films on either side of the MQWs, and, thus, could be used for the development of an electrically pumped deep-ultraviolet laser by further optimizing the structures.

Index Terms: Ultraviolet, AlGaN, GRINSCH, amplified spontaneous emission, polarization doping, quantum well.

1. Introduction

The development of deep-ultraviolet (DUV) semiconductor lasers has been an active area of research over the past several years, motivated by a large number of potential applications [1]. Such applications include free space non-line-of-sight communications, fluorescence or Raman identification of chemical and biological agents, and medical diagnostic applications [2]. A number

of groups have demonstrated stimulated emission and prototypes of optically pumped DUV lasers based on $Al_xGa1_{-x}N$ multiple quantum well (MQW) structures [3]–[10]. Some of these devices were grown on AlN template on sapphire [3]–[6] and others on AlN substrates [7], [8]. Our group has demonstrated a maximum net modal gain of 120 cm^{-1} at a transparency threshold of 5 $\mu J/cm^2$, corresponding to 1.4 $\times$ 10^{17} cm^{-3} excited carriers in DUV emitting AlGaN MQWs, grown on 6H-SiC substrates by plasma-assisted molecular beam epitaxy (PAMBE) [9]. This threshold value is about two orders of magnitude less than that calculated for identical but homogeneous AlGaN MQWs [10], a result attributed to a growth mode, which introduces deep band-structure potential fluctuations in the AlGaN wells [9], [10].

The development of electrically pumped DUV semiconductor lasers is lagging, due to the difficulty in doping AlGaN films with high AlN mole fraction p-type because of the high ionization energies of Mg-acceptors, which are on the order of 630 meV for AlN [11]. The reported shortest wavelengths of electrically pumped UV lasers are 342 and 336nm with threshold currents of 8 kA/cm^2 and 17 kA/cm^2, respectively [12], [13]. Recently, researchers reported ultralow threshold electrically injected AlGaN nanowire-based UV lasers emitting at 239 nm on Si substrate, a result attributed to higher crystalline quality and improved p-type doping efficiency of AlGaN nanowires [14]. Thus, any breakthrough in developing an electrically pumped DUV semiconductor laser will depend on the ability to dope efficiently high Al content AlGaN p-type alloys on less defective templates (AlN etc) [15]. An alternative approach to homogeneous doping of AlGaN alloys is the polarization enhanced doping in compositionally graded AlGaN alloys [16], [17]. In this method, 3D mobile carriers can be produced with the aid of polarization charges in graded AlGaN structures without the need of intentional impurities. Application of this polarization enhanced p-type doping of AlGaN layers has already been implemented in light emitting diodes (LEDs) using compositionally graded $Al_xGa_{1-x}N$ alloys with small AlN mole fraction ($x < 0.3$) [18]–[20].

A semiconductor laser design, which can take advantage of the polarization-enhanced p-type doping in compositionally graded AlGaN alloys, is a structure having the graded-index separate confinement heterostructure (GRINSCH) configuration. Such a laser design has been implemented successfully in traditional cubic III-V compounds, for example, GaAs and InP-based lasers. In these structures, the refractive index profile of wave guiding layers were graded either in a parabolic or linear profile to obtain confinement of the optical mode. Such designs led to lasers operating at very low current thresholds [21]–[23]. It should be stressed that due to their cubic symmetry, polarization-enhanced doping is not present in the compositionally graded wave guiding layers of the GRINSCH structures based on traditional III-V compounds. Recently, GRINSCH-based InGaN laser diodes were demonstrated with low threshold current density of 3.5 kA/cm^2 [24], [25]. Numerically, the GRINSCH InGaN MQW laser diode showed better optical performance than the conventional step-index structure [26]. Normally the p-type doping is not a challenge for the InGaN-based laser diode. Thus, the authors did not intentionally take advantage of the compositionally graded $In_xGa_{1-x}N$ layer in designing their laser diodes.

Our group has previously reported the growth and fabrication of DUV emitters based on AlGaN double heterostructure in a GRINSCH configuration, where the active region was a 75 nm thick AlGaN film [27]. This device emitting at 257 nm was found to have a net optical gain of 80 cm^{-1} at relative low transparency threshold of 14 $\mu J/cm^2$ under femtosecond laser pumping [28]. In general, MQWs based lasers were demonstrated to have a much lower threshold current density compared with double heterostructure [12], [21]. Therefore, to achieve high-performance DUV laser devices, we have to optimize the active region to find the optimum number of quantum wells in such devices. This topic was addressed both theoretically [29], [30], and experimentally [31], in InGaN/GaN MQWs for both LEDs and laser devices. Also, there are some numerical studies on the optimization of GaN/AlGaN MQW-based laser structures emitting at wavelengths longer than 300 nm [32]–[34]. In this paper, we report the development of $Al_xGa_{1-x}N/Al_yGa_{1-y}N$ MQW-based DUV emitters having a GRINSCH design, grown on 6H-SiC substrates. Particular emphasis is placed on identifying the effect of the number of $Al_xGa_{1-x}N/Al_yGa_{1-y}N$ QWs on threshold properties of DUV emitters.

TABLE 1
GRINSCH Devices With 1, 2 and 10 QWs

First graded layer	MQWs (active region)	Second graded layer	Cap
50 nm AlN - $Al_{0.8}Ga_{0.2}N$	1 QW 1.5 nm $Al_{0.65}Ga_{0.35}N$/3 nm $Al_{0.8}Ga_{0.2}N$	50 nm $Al_{0.8}Ga_{0.2}N$-AlN	50 nm AlN
50 nm AlN - $Al_{0.8}Ga_{0.2}N$	2 QWs 1.5 nm $Al_{0.65}Ga_{0.35}N$/3 nm $Al_{0.8}Ga_{0.2}N$	50 nm $Al_{0.8}Ga_{0.2}N$-AlN	50 nm AlN
50 nm AlN - $Al_{0.8}Ga_{0.2}N$	10 QWs 1.5nm $Al_{0.65}Ga_{0.35}N$/3 nm $Al_{0.8}Ga_{0.2}N$	50 nm $Al_{0.8}Ga_{0.2}N$-AlN	50 nm AlN

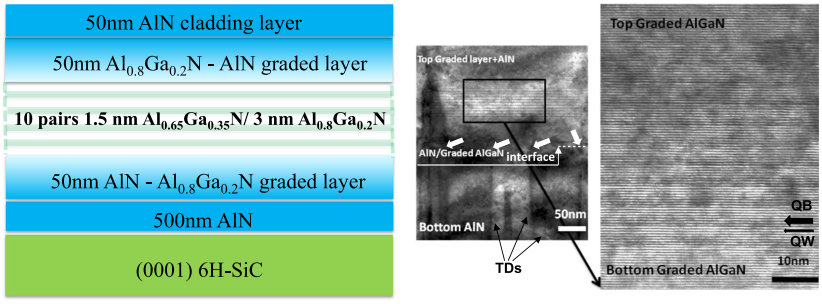

Fig. 1. (a) Schematic of the investigated GRINSCH device with 10 pairs of AlGaN MQWs; (b) TEM cross-sectional micrograph of this device. The dark arrows indicated TDs, white dash line indicated the AlN/graded AlGaN layer interface and the white arrows exhibited the termination/bending of TDs at the AlN/graded AlGaN layer interface; (c) enlarged image of the active region of the device with black arrows for the position of QW (small black arrow) and QB (large black arrow).

2. Experimental Methods

The structures of the three investigated samples, shown in Table 1, are identical except for the number of QWs. The active region consists of 1, 2, and 10 pairs of 1.5 nm $Al_{0.65}Ga_{0.35}N$/3 nm $Al_{0.8}Ga_{0.2}N$ MQWs. The composition of the graded AlGaN films on either side of the active region varies linearly from AlN to $Al_{0.8}Ga_{0.2}N$ and from $Al_{0.8}Ga_{0.2}N$ to AlN. The device with the 10 MQWs is shown schematically in Fig. 1(a).

All samples were grown on the (0001) Si-face of 6H-SiC by PAMBE. Growth of AlGaN based emitters on SiC has several advantages. The lattice mismatch between SiC and AlN is only 1%. Other advantages include the high thermal conductivity of SiC compared to that of sapphire, the ability to form facets by cleaving and to facilitate hole injection by doping the SiC p-type. The MBE system is equipped with a Veeco RF plasma source for nitrogen activation and traditional effusion cells for the evaporation of Al, Ga, and In. The substrate preparation and film growth were monitored by reflection high-energy electron diffraction (RHEED) at 10 keV electron energy. The SiC substrates were first cleaned *ex situ* in organic solvents followed by dipping into heated piranha etch and then buffered HF to remove surface contaminants and oxides. Also, the substrates were cleaned *in situ* by exposure to Ga flux at 750 °C for complete Ga coverage followed by fast heating to 850 °C for Ga desorption. This process was found to lead to a streaky RHEED pattern, which is attributed to the removal of oxygen, carbon, hydrogen, and other physisorbed or chemisorbed impurities through the formation of volatile Ga-compounds. The substrate temperature during growth of the AlGaN QWs and the AlGaN graded regions was kept at 780 °C. The growth of the wells in the various devices was done under excess Ga than that required for stoichiometric growth, which, as discussed elsewhere, leads to band-structure potential fluctuations [35]–[37]. Such fluctuations

lead to stimulated emissions at threshold pumping powers that are significantly lower than those in homogeneous materials [9], [10], [27], [28].

The microstructure of the devices was studied by transmission electron microscopy (TEM). The TEM specimens were prepared by standard mechanical polishing followed by ion-beam-thinning at 4.5 keV. Conventional diffraction-contrast images and high-resolution phase contrast images were recorded with a JEM 4000EX high-resolution electron microscope equipped with a top-entry, double tilt specimen holder operated at 400 keV [38].

The optical properties of these samples were investigated under femtosecond optical pumping. The samples were excited with 220 nm, 150 fs laser pulses obtained by pumping a proper crystal (Spectra Physics GWU-24FL) with a mode-locked ultra-fast high-power Ti:sapphire laser (Spectra Physics MaiTai, 82 MHz) operating at 880 nm. The laser pulses were focused on the sample surface through a cylindrical lens. The pumping fluence on the sample was varied up to 80 μJ/cm^2. The photoluminescence (PL) was collected from the cleaved edge of the sample through a UV-transmitting objective, a UV-transmitting movable analyzer, a computer-controlled f/4 monochromator (Cornerstone 260) with UV-efficient gratings, and a lock-in amplifier (Oriel Merlin) coupled to a UV-optimized photomultiplier tube (Oriel Instruments 77348).

To account for the experimental data, the optical properties including optical threshold pumping power in samples with different number of QWs were calculated by using a commercially available software package called Laser Technology Integrated Program (LASTIP) provided by Crosslight Software Inc. In LASTIP, the software combines QW band structure calculations using the 6 x 6 k.p model, radiative and nonradiative carrier recombination, wave guiding and optical gain calculations [29], [30], [32], [39], [40]. In the simulation setup, we used the self-consistent MQW/Piezo module which includes the built-in polarization-induced fields by the spontaneous and piezoelectric polarization in the band diagram calculation [41]. We also used the Advanced Optics/Pumped laser module to simulate the optical pumping conditions, using material parameters for the AlGaN alloys from the literature [42], [43]. The program follows the gain/absorption theory presented by Chuang [41]. LASTIP uses a sampling (1D cut) of the potential from the drift-diffusion mesh to solve the Schrodinger equation for the AlGaN QW. The obtained wavefunctions are used in the Fermi golden rule calculations to compute the gain and the density profiles in the drift-diffusion model under optical pumping. This is the part that incorporates the effect of the piezo charges induced by the strong polarizations mentioned earlier. More detail description of the physical models that are used in LASTIP simulations can be found in refs. [42]–[45].

3. Results and Discussion

3.1 Film Microstructure

Fig. 1(b) shows a cross-sectional electron micrograph of the sample. The high density of threading dislocations (TDs), formed at the interface between AlN and SiC, propagate along the growth direction. However, many of the TDs terminated/bent at the AlN/graded AlGaN layer (white arrows). As indicated in the enlarged image of Fig. 1(c), the $Al_{0.65}Ga_{0.35}N/Al_{0.8}Ga_{0.2}N$ MQWs were well-formed with relatively abrupt interfaces [37], [38].

3.2 Optical Properties

Fig. 2(a) shows the photoluminescence (PL) spectra at room temperature, measured at 10 μJ/cm^2, of the GRINSCH devices, whose active region consists of 1, 2 and 10 pairs of $Al_{0.65}Ga_{0.35}N/Al_{0.8}Ga_{0.2}N$ MQWs. The spectra undergo a small blue shift from 275 to 272 nm as the number of QWs increases from 1 to 10. A similar shift was also reported in the PL investigation of InGaN/GaN MQWs [31] and was attributed to the piezoelectric fields and strain relaxation as the number of InGaN QWs increases. The inset of Fig. 2(a) indicates that the emission intensity increases linearly with the number of the wells, a result consistent with theoretical predictions in quantum well lasers [46].

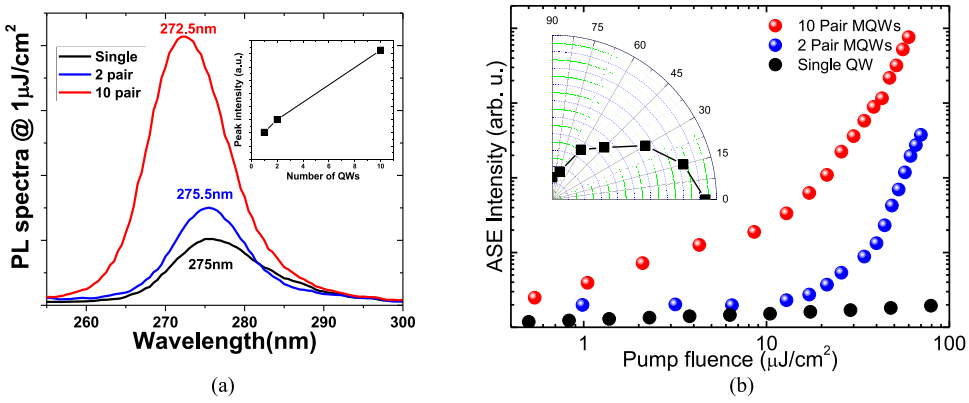

Fig. 2. (a) Room-temperature PL spectra from of three GRINSCH devices, whose active region consists of 1, 2 and 10 pairs of $Al_{0.65}Ga_{0.35}N/Al_{0.8}Ga_{0.2}N$ MQWs. The data in the insert of the figure indicate that the emission intensity increases linearly with the number of the wells; (b) The ASE peak intensity as a function of the pump fluence for the three samples. Inset image shows the polar plot of the peak intensity as a function of the analyzer angle for the sample with 10 MQWs.

Fig. 2(b) shows the room-temperature PL peak intensity as a function of pump fluence for the three samples. As seen from these data, the dependence is linear for the sample with a single QW (SQW), while the intensity shows superlinear behavior with increasing pumping fluence for the samples with 2 and 10 pairs of QWs. The superlinear behavior provided a strong evidence of stimulated emission. Similarly, lasing was not observed for a single QW InGaN laser structure [31]. From the Fig. 2(b), we estimate that the transparency threshold is 25 μJ/cm^2 and 6 μJ/cm^2 for the samples with two and ten pairs of QWs, respectively. Such relatively low threshold pumping power densities were attributed to deep band-structure potential fluctuations introduced in AlGaN films, grown under Ga-rich condition, as discussed previously [9], [10], [28]. The observed threshold pumping power of 6 μJ/cm^2 is lower than the 14 μJ/cm^2 measured in a GRINSCH structure whose active region consists of a bulk AlGaN film [28].

We have also investigated the polarization properties of the amplified spontaneous emission (ASE) to better understand the origin of the observed PL. The inset image in Fig. 2(b) shows the polar plot of the peak intensity as a function of the analyzer angle for the sample with 10 MQWs. "0°" corresponds to TM polarization of the emission (where the electric field vector of the emitted light is perpendicular to the QW plane) and 90° corresponds to TE polarization (where the electric field vector of the emitted light is parallel to the QW plane). Intensities have been recorded at the highest pump fluence (60 μJ/cm^2) and they were reported on a linear scale. Thus, the emission from this GRINSCH structure was strongly TM polarized. It is well-known that the ASE polarization in AlGaN materials depends on a number of parameters, such as the Al content, the strain in the active layer, and the thicknesses of the wells and barriers [47]. In particular, a turnover from the TE to the TM polarization is expected for an Al content of 60-80%, depending on the actual device structure [48]–[50]. Thus, our result is consistent with what has been reported in the literature for AlGaN MQWs of similar Al composition [4].

3.3 Optical Simulations

The confinement of the optical mode in the investigated GRINSCH structures was determined using the index of refraction values for the AlGaN alloys with different compositions obtained from Brunner *et al.* [51]. Fig. 3(a) shows the vertical profile of the index of refraction and the TM optical mode profile for the GRINSCH device with 10 MQWs. The black curve in Fig. 3(b) shows the calculated dependence of the optical confinement factor as a function of the number of QWs under the fundamental waveguide mode. According to these data, the optical confinement factor increases linearly as the number of QWs increases from 1 to 10, and it appears to saturate as the number

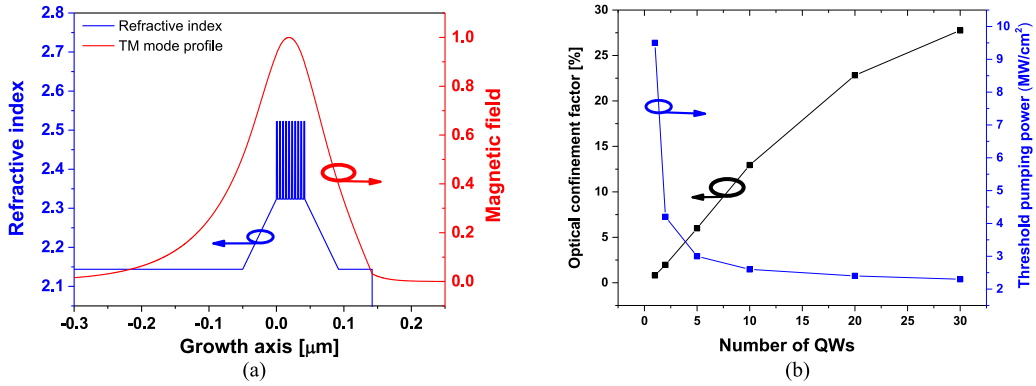

Fig. 3. (a) Vertical profile of the index of refraction and the TM optical mode profile for the GRINSCH device with 10 MQWs; (b) the calculated dependence of the optical confinement factor as a function of the number of QWs (black curve) and the threshold pumping power versus the number of QWs in the active region (blue curve).

of QWs increases further. These data show clearly the benefits of designing an AlGaN-based DUV laser in the GRINSCH configuration rather than using only AlGaN MQWs, whose optical confinement factor is much smaller [13], [14], [33], [34].

The black curve in Fig. 3(b) indicates that better optical confinement of the optical mode requires a large number of QWs. However, other factors are also important in determining the optimum number of QWs to achieve a high-performance laser. The effect of the number of $Al_{0.65}Ga_{0.35}N/Al_{0.8}Ga_{0.2}N$ MQWs on the threshold pumping power was simulated using the advanced LASTIP software package as discussed earlier. The blue curve in Fig. 3(b) shows the threshold pumping power density of AlGaN-based GRINSCH-MQW lasers as a function of the number of QWs. According to these data, better laser performance requires that the number of QWs must be more than five. Thus, the optimized number of QWs for 1.5 nm $Al_{0.65}Ga_{0.35}N$/3nm $Al_{0.8}Ga_{0.2}N$ GRINSCH lasers is found to be 5–10. This number is also consistent with recent experimental reports from AlGaN MQW-based DUV lasers [3]–[8]. The reported lasers with fewer QWs [5] required significant higher threshold pumping power than lasers having more than five pairs of MQWs [3], [4], [6]–[8]. Thus, our experimental results are qualitatively in agreement with the simulated results.

3.4 Band Structure

The energy band diagram of the device, described in Fig. 1(a), was found by solving self-consistently the Schrodinger and Poisson's equations and the results are shown in Fig. 4(a) [52]. As discussed earlier, these calculations were performed using a commercially available software package (Crosslight LASTIP). This band diagram clearly indicates the formation of a *p-n* junction due to polarization p- and n-type doping of the AlGaN graded layers on either side of the active region [16]–[20], [27], [28], [37]. Shown in the same figure are also the concentration of holes and electrons induced by polarization. Such high concentration of electrons and holes ($\sim 3 \times 10^{18}\,cm^{-3}$) in the p-n junction without the utilization of intentional impurities implies that this GRINSCH structure has the potential for the development of electrically pumped DUV laser. This doping level in both sides of the junction assumes the existence of a sufficient amount of acceptor-like or donor-like impurities or defects in either side of the junction, which can be ionized by polarization. Such impurities or defects may occur naturally during the growth process or may be introduced intentionally by incorporating p-type dopants in the first AlGaN compositionally graded layer and n-type dopants in the second AlGaN compositionally graded layer [53].

Fig. 4(b) and (c) illustrate schematically how the two compositionally graded $Al_xGa_{1-x}N$ films ($0.8 \leq x \leq 1$) in the investigated devices are doped by polarization p-type (bottom $Al_xGa_{1-x}N$ film) and n-type (top $Al_xGa_{1-x}N$ film) [20]. Fig. 4(b) shows the compositional variation of the two

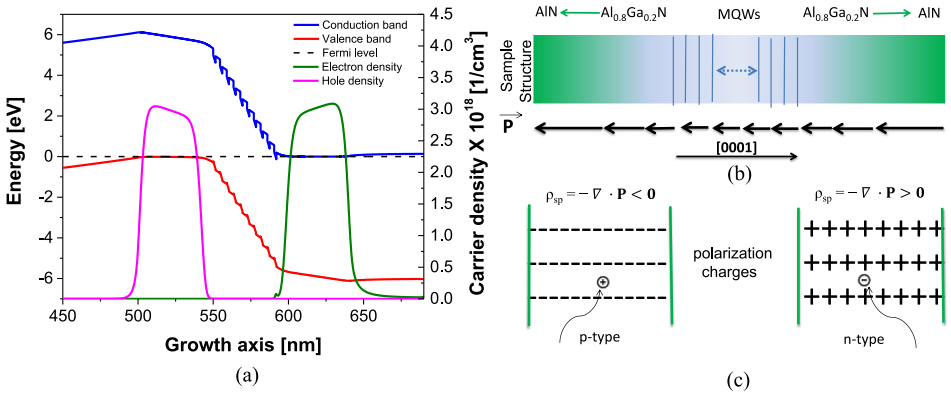

Fig. 4. (a) Simulated energy band diagram of the GRINSCH AlGaN structure with 10 MQWs under thermal equilibrium and its electron and hole concentrations in compositionally graded AlGaN layers. (b) Schematic illustration of AlGaN compositional grading and variation of the magnitude and direction of the polarization vector relative to the growth direction. (c) Polarization-induced n- and p-type doping in two compositionally graded AlGaN films.

$Al_xGa_{1-x}N$ films, the [0001] direction of growth (Ga-polar), and the direction and variation of the magnitude of the total polarization vector, which results from the addition of the spontaneous and piezoelectric polarization in the two compositionally graded $Al_xGa_{1-x}N$ films. Fig. 4(c) shows schematically how polarization leads to p- and n-type doping of the bottom and top AlGaN compositionally graded layers, respectively. Specifically, compositional grading of $Al_xGa_{1-x}N$ from $x = 1$ to 0.8 along the [0001] direction leads to negative polarization charges, resulting in p-type doping of the film through polarization-assisted ionization of various acceptor-like impurities or defects. Similarly, linear grading of $Al_xGa_{1-x}N$ in the reverse direction, $x = 0.8$ to 1, creates positive polarization charges, resulting in n-type doping of the film through polarization-assisted ionization of donor-like impurities or defects. The density of the polarization charges is related to the spatial variation of the total electric polarization vector **P** and can be calculated from the expression $\rho_{pol} = -\nabla \cdot \mathbf{P}$. Thus, the polarization charge density depends on the degree of compositional grading and thickness of the graded AlGaN film.

Certain modifications are required in the discussed GRINSCH device for electrical injection. First, we address the issue of hole injection and low resistance p-type Ohmic contact to the proposed GRINSCH device. We believe this problem can be addressed by growing the device on degenerately doped p-SiC substrates, which are commercially available. The formation of Ohmic contacts to such substrate is well known. Furthermore, due to the inverted geometry (p-down) the hole injection to QWs is facilitated by the internal fields due to polarization. Regarding the formation of low resistance Ohmic contact to AlN, the proposed device can be modified to emit at slightly longer wavelengths by making the top layer out of the $Al_{0.8}Ga_{0.2}N$ layer. We have demonstrated previously that the n-type $Al_{0.8}Ga_{0.2}N$ films can be doped degenerately and we were able to form Vanadium-based Ohmic contact with contact resistivity 10^{-4} (Ohm.cm^2) [54], [55].

4. Summary and Conclusion

In summary, we have investigated the growth by PAMBE and characterizations of DUV emitting structures based on AlGaN MQWs in the form of GRINSCH configuration. TEM studies of these devices indicate that the first compositionally graded AlGaN film might also be serving as a strain transition buffer, by blocking threading defects in the vicinity of the AlN/AlGaN heterointerface, resulting in a reduction of the TDs in the active layer. Optical pumping of these devices indicates that it requires more than single QW to observe amplified spontaneous emission. This result is qualitatively consistent with simulated results of the dependence of the confinement factor of the

optical mode and transparency threshold as a function of the number of the AlGaN MQWs. Finally, the calculation of the band diagram of these devices indicates the formation of a p-n junction due to polarization doping of the compositionally graded AlGaN alloys on either side of the MQWs with a concentration of free electrons and holes of about 3×10^{18} cm^{-3}. Thus, the proposed GRINSCH structure could be used for the development of an electrically pumped deep-ultraviolet laser by further optimizing the structures.

Acknowledgment

The authors would like to thank Prof. D. J. Smith of Arizona State University for the electron microscopy results.

References

[1] A. Khan, K. Balakrishnan, and T. Katona, "Ultraviolet light-emitting diodes based on group three nitrides," *Nature Photon.*, vol. 2, no. 2, pp. 77–84, 2008.
[2] T. D. Moustakas, "Ultraviolet optoelectronic devices based on AlGaN alloys grown by molecular beam epitaxy," *MRS Commun.*, vol. 6, no. 3, pp. 247–269, 2016.
[3] Y. Tian *et al.*, "Stimulated emission at 288 nm from silicon-doped AlGaN-based multiple-quantum-well laser," *Opt. Exp.*, vol. 23, pp. 11334–11340, 2015.
[4] X. Li *et al.*, "Demonstration of transverse-magnetic deep-ultraviolet stimulated emission from AlGaN multiple-quantum-well lasers grown on a sapphire substrate," *Appl. Phys. Lett.*, vol. 106, p. 041115, 2015.
[5] J. Jeschke *et al.*, "UV-C lasing from AlGaN multiple quantum well on different types of AlN/sapphire templates," *IEEE Photon. Technol. Lett.*, vol. 27, no. 18, pp. 1969–1972, Sep. 2015.
[6] F. Asif *et al.*, "Deep ultraviolet photopumped stimulated emission from partially relaxed AlGaN multiple quantum well heterostructures grown on sapphire substrates," *J. Vac. Sci. Technol. B*, vol. 32, no. 6, p. 061204, 2014.
[7] M. Lachab *et al.*, "Optical polarization control of photo-pumped stimulated emissions at 238 nm from AlGaN multiple-quantum-well laser structures on AlN substrates," *Appl. Phys. Exp.*, vol. 10, p. 012702, 2017.
[8] Z. Bryan, I. Bryan, S. Mita, J. Tweedie, Z. Sitar, and R. Collazo, "Strain dependence on polarization properties of AlGaN and AlGaN-based ultraviolet lasers grown on AlN substrates," *Appl. Phys. Lett.*, vol. 106, p. 232101, 2015.
[9] E. F. Pecora *et al.*, "Sub-250 nm room-temperature optical gain from AlGaN/AlN multiple quantum wells with strong band-structure potential fluctuations," *Appl. Phys. Lett.*, vol. 100, p. 061111, 2012.
[10] E. F. Pecora *et al.*, "Sub-250 nm light emission and optical gain in AlGaN materials," *J. Appl. Phys.*, vol. 113, p. 013106, 2013.
[11] Y. Taniyasu, M. Kasu, and T. Makimoto, "An aluminium nitride light-emitting diode with a wavelength of 210 nanometres," *Nature*, vol. 441, pp. 325–328, 2006.
[12] H. Yoshida, Y. Yamashita, M. Kuwabara, and H. Kan, "A 342-nm ultraviolet AlGaN multiple-quantum-well laser diode," *Nature Photon.*, vol. 2, no. 9, pp. 551–554, 2008.
[13] H. Yoshida, Y. Yamashita, M. Kuwabara, and H. Kan, "Demonstration of an ultraviolet 336 nm AlGaN multiple-quantum-well laser diode," *Appl. Phys. Lett.*, vol. 93, p. 241106, 2008.
[14] S. Zhao, X. Liu, Y. Wu, and Z. Mi, "An electrically pumped 239 nm AlGaN nanowire laser operating at room temperature," *Appl. Phys. Lett.*, vol. 109, p. 191106, 2016.
[15] H. Sun *et al.*, "Influence of TMAl preflow on AlN epitaxy on sapphire," *Appl. Phys. Lett.*, vol. 110, p. 192106, 2017.
[16] Z. Liu *et al.*, "Impurity resonant states p-type doping in wide-band-gap nitrides," *Sci. Rep.*, vol. 6, 2016, Art. no. 19537.
[17] A. V. Kuchuk *et al.*, "Nanoscale electrostructural characterization of compositionally graded $Al_xGa_{1-x}N$ heterostructures on GaN/sapphire (0001) substrate," *ACS Appl. Mater. Interfaces*, vol. 7, pp. 23320–23327, 2015.
[18] S. D. Carnevale, T. F. Kent, P. J. Phillips, M. J. Mills, S. Rajan, and R. C. Myers, "Polarization-induced pn diodes in wide-band-gap nanowires with ultraviolet electroluminescence," *Nano Lett.*, vol. 12, no. 2, pp. 915–920, 2012.
[19] S. Li *et al.*, "Polarization doping: Reservoir effects of the substrate in AlGaN graded layers," *J. Appl. Phys.*, vol. 112, p. 053711, 2012.
[20] H. Sun and T. D. Moustakas, "UV emitters based on an AlGaN p–n junction in the form of graded-index separate confinement heterostructure," *Appl. Phys. Exp.*, vol. 7, p. 012104, 2014.
[21] W. T. Tsang, "Extremely low threshold (AlGa) As modified multi quantum well heterostructure lasers grown by molecular-beam epitaxy," *Appl. Phys. Lett.*, vol. 39, no. 10, pp. 786–788, 1981.
[22] W. T. Tsang, "Extremely low threshold (AlGa) As graded-index waveguide separate-confinement heterostructure lasers grown by molecular beam epitaxy," *Appl. Phys. Lett.*, vol. 40, no. 3, pp. 217–219, 1982.
[23] D. Kasemset, C.-S. Hong, N. B. Patel, and P. D. Dapkus, "Graded barrier single quantum well lasers—Theory and experiment," *IEEE J. Quantum Electron.*, vol. 19, no. 6, pp. 1025–1030, Jun. 1983.
[24] S. Stańczyk *et al.*, "Graded-index separate confinement heterostructure InGaN laser diodes," *Appl. Phys. Lett.*, vol. 103, p. 261107, 2013.
[25] A. Kafar *et al.*, "Nitride superluminescent diodes with broadened emission spectrum fabricated using laterally patterned substrate," *Opt. Exp.*, vol. 24, pp. 9673–9682, 2016.
[26] J. A. Martin and M. Sanchez, "Comparison between a graded and setp-index optical cavity in InGaN MQW laser diodes," *Semicond. Sci. Technol.*, vol. 20, pp. 290–295, 2005.

[27] H. Sun *et al.*, "Development of AlGaN-based graded-index-separate-confinement heterostructure deep UV emitters by molecular beam epitaxy," *J. Vac. Sci. Technol. B*, vol. 31, pp. 03C117-1–03C117-7, 2013.
[28] E. F. Pecora, H. Sun, L. Dal Negro, and T. D. Moustakas, "Deep-UV optical gain in AlGaN-based graded index separate-confinement heterostructure," *Opt. Mater. Exp.*, vol. 5, pp. 809–817, 2015.
[29] C. S. Xia *et al.*, "Optimal number of quantum wells for blue InGaN/GaN light-emitting diodes," *Appl. Phys. Lett.*, vol. 100, no. 26, p. 263504, 2012.
[30] Y. P. Zhang *et al.*, "Nonradiative recombination—Critical in choosing quantum well number for InGaN/GaN light-emitting diodes," *Opt. Exp.*, vol. 23, pp. A34–A42, 2015.
[31] M. S. Minsky *et al.*, "Characterization of high-quality InGaN/GaN multiquantum wells with time-resolved photoluminescence," *Appl. Phys. Lett.*, vol. 72, p. 1066, 1998.
[32] J.-R. Chen *et al.*, "Numerical study on optimization of active layer structures for GaN/AlGaN multiple-quantum-well laser diodes," *J. Lightw. Technol.*, vol. 26, no. 17, pp. 3155–3165, Sep. 2008.
[33] K. A. Bulashevich, M. S. Ramm, and S. Yu. Karpov, "Effects of electron and optical confinement on performance of UV laser diodes," *Phys. Status Solidi C*, vol. 6, pp. 603–606, 2009.
[34] A. J. Ghazai, S. M. Thahab, H. A. Hassan, and Z. Hassan, "The effects of quantum wells number and the built-in polarization on the performance of quaternary AlInGaN UV laser diode," *Optik*, vol. 123, pp. 856–859, 2012.
[35] T. D. Moustakas *et al.*, "Deep UV-LEDs with high IQE based on AlGaN alloys with strong band structure potential fluctuations," *Proc. SPIE*, vol. 8278, 2012, Art. no. 82780L-1.
[36] W. Zhang *et al.*, "Molecular beam epitaxy growth of AlGaN quantum wells on 6H-SiC substrates with high internal quantum efficiency," *J. Vac. Sci. Technol. B*, vol. 30, pp. 02B119-1–02B119-5, 2012.
[37] H. Sun, E. F. Pecora, J. Woodward, D. J. Smith, L. Dal Negro, and T. D. Moustakas, "Effect of indium in $Al_{0.65}Ga_{0.35}N/Al_{0.8}Ga_{0.2}N$ MQWs for the development of deep-UV laser structures in the form of graded-index separate confinement heterostructure (GRINSCH)," *Phys. Status Solidi A*, vol. 213, pp. 1165–1169, 2016.
[38] A. Boley, H. Sun, M. R. McCartney, D. J. Smith, and T. D. Moustakas, "Characterization of AlGaN-based GRINSCH using TEM and electron holography," *Microsc. Microanal.*, vol. 19, Suppl. 2, pp. 1382–1383, 2013.
[39] F. Wu *et al.*, "Significant internal quantum efficiency enhancement of GaN/AlGaN multiple quantum wells emitting at ~350 nm via step quantum well structure design," *J. Phys. D, Appl. Phys.*, vol. 50, p. 245101, 2017.
[40] W. W. Chow, M. Kneissl, J. E. Northrup, and N. M. Johnson, "Influence of quantum-well-barrier composition on gain and threshold current in AlGaN lasers," *Appl. Phys. Lett.*, vol. 90, p. 101116, 2007.
[41] S. L. Chuang, *Physics of Photonic Devices*, 2nd ed. New York, NY, USA: Wiley, 2009.
[42] J. Piprek, *Nitride Semiconductor Devices: Principles and Simulation*. Berlin, Germany: Wiley-VCH Verlag, 2007.
[43] Y. K. Kuo, S. H. Yen, and J. R. Chen, "Ultraviolet light-emitting diodes," in *Nitride Semiconductor Devices: Principles and Simulation*. Berlin, Germany: Wiley-VCH Verlag, 2007.
[44] P. Yeh, *Optical Waves in Layered Media*. New York, NY, USA: Wiley Interscience, 1988.
[45] J. Piprek and S. Li, "GaN-based light-emitting diodes," in *Optoelectronic Devices: Advanced Simulation and Analysis*. New York, NY, USA: Springer Verlag, 2005.
[46] Y. Arakawa and A. Yariv, "Quantum well lasers–Gain, spectra, dynamics," *IEEE J. Quantum Electron.*, vol. 22, no. 9, pp. 1887–1899, Sep. 1986.
[47] J. E. Northrup *et al.*, "Effect of strain and barrier composition on the polarization of light emission from AlGaN/AlN quantum wells," *Appl. Phys. Lett.*, vol. 100, no. 2, p. 021101, 2012.
[48] J. Zhang, H. Zhao, and N. Tansu, "Effect of crystal-field split-off hole and heavy-hole bands crossover on gain characteristics of high Al-content AlGaN quantum well lasers," *Appl. Phys. Lett.*, vol. 97, no. 11, p. 111105, 2010.
[49] A. A. Yamaguchi, "Theoretical investigation of optical polarization properties in Al-rich AlGaN quantum wells with various substrate orientations," *Appl. Phys. Lett.*, vol. 96, no. 15, p. 151911, 2010.
[50] S. Park, "Al composition dependence of the optical gain characteristics of a-plane Al-rich AlGaN/AlN quantum-well structures," *J. Korean Phys. Soc.*, vol. 59, pp. 357–361, 2011.
[51] D. Brunner *et al.*, "Optical constants of epitaxial AlGaN films and their temperature dependence," *J. Appl. Phys.*, vol. 82, p. 5090, 1997.
[52] B. Janjua *et al.*, "Droop-free $Al_xGa_{1-x}N/Al_yGa_{1-y}N$ quantum-disks-in-nanowires ultraviolet LED emitting at 337 nm on metal/silicon substrates," *Opt. Exp.*, vol. 25, no. 2, pp. 1381–1390, 2017.
[53] B. Janjua *et al.*, "Self-planarized quantum-disks-in-nanowires ultraviolet-B emitters utilizing pendeo-epitaxy," *Nanoscale*, vol. 9, pp. 7805–7813, 2017, doi: 10.1039/C7NR00006E.
[54] T. Xu, C. Thomidis, I. Friel, and T. D. Moustakas, "Growth and silicon doping of AlGaN films in the entire alloy composition by molecular beam epitaxy," *Phys. Status Solidi C*, vol. 2, no. 7, pp. 2220–2223, 2005.
[55] R. France, T. Xu, P. Chen, R. Chandrasekaran, and T. D. Moustakas, "Vanadium-based ohmic contacts to n-AlGaN in the entire alloy composition," *Appl. Phys. Lett.*, vol. 90, p. 062115, 2007.